Effect of external confinement on Alkali-Silica Reaction (ASR)-induced expansion and damage

Andisheh Zahedi [(1)], Nusrat Zubaida [(2)], Leandro Sanchez [(3)], Patrice Rivard [(4)]

(1) PhD Candidate, Civil Engineering, University of Ottawa, Ottawa, Canada, azahe049@uottawa.ca

(2) MASc Candidate, Civil Engineering, University of Ottawa, Ottawa, Canada, nzuba086@uottawa.ca

(3) Associate Professor, Civil Engineering, University of Ottawa, Ottawa, Canada, leandro.sanchez@uottawa.ca

(4) Full Professor, Civil Engineering, University of Sherbrooke, Sherbrooke, Canada, patrice.rivard@usherbrooke.ca

Abstract

Recently, a number of research studies have focused on the understanding of alkali-silica reaction (AAR) induced expansion and damage (i.e. cracks initiation and propagation) and its impact on the mechanical properties of affected concrete. Literature data shows that ASR cracks are predominantly generated within the aggregates particles and propagate to the cement paste as a function of induced expansion and development. Moreover, significant impact on tensile strength and modulus of elasticity is observed for ASR-affected concrete. Yet, most of the current results found were obtained under a non-confined (i.e. free expansion) state which does not represent what happens in the field. Often, concrete structures are under a 2D or 3D confinement state which likely makes their deterioration process different from the ones obtained under unconfined states in the laboratory. This research aims to study the influence of distinct external confinement scenarios on ASR-induced expansion and damage. Concrete samples incorporating two different highly reactive aggregates and confined with three distinct amounts of carbon fibre reinforced polymer (CFRP) were fabricated and monitored in the laboratory. Four levels of expansion (i.e. 0.05%, 0.12%, 0.20% and 0.30%) were selected to perform non-destructive (NIRAS test) and microscopic (Damage Rating Index) test procedures. Comparisons amongst the results obtained from distinct confinement scenarios were performed and recommendations on the use of unconfined tests for evaluation ASR structural implications were conducted.

Keywords: *alkali aggregate reaction (AAR); confinement effects; CFRP; expansion; reactive aggregate*

1. INTRODUCTION

Alkali-silica reaction (ASR), one of the most deleterious mechanisms affecting the durability of concrete infrastructure around the world, is a chemical reaction between the alkalis (Na^+, K^+, and OH^-) from the concrete pore solution and non-crystallized siliceous phases of the aggregates used in concrete. ASR provides a gel that swells in the presence of water leading to important tensile stresses and cracking in affected concrete [1].

One of the biggest challenges while dealing with critical ASR-affected infrastructure is determining the induced expansion and damage attained to date in the different locations of the structure (i.e. diagnosis), to forecast its potential for further distress over time (i.e. prognosis), as well as its potential structural implications [2]. Recently, a number of research studies have demonstrated that ASR strongly influences the mechanical properties of affected concrete, especially its tensile strength and modulus of elasticity, where important losses of about 85% and 50% were measured, respectively, for very high expansion levels [3, 4]. However, most of the current results found in the literature were obtained under a non-confined (i.e. free-expansion) state which does not represent what actually happens within a real structure. Often, concrete structures are under a 2D or 3D confinement state in the field which likely makes their deterioration process different from the ones obtained under unconfined states in the laboratory. Therefore, some questions can be raised in that regard such as: a) what is the difference between the loss of mechanical properties in confined vs unconfined conditions?; b) how to intepret/use the results obtained from cores extracted from ASR-affected members in the reassessment of affected structures? and c) how to interprete/use the results from cores as input for numerical/analytical models to predict the future behaviour of affected structures? This work aims to evaluate the effect of external confinement on ASR-induced expansion and damage, trying to answer at least partially some of the aforementioned questions.

2. CONFINEMENT EFFECT ON ASR-INDUCED DEVELOPMENT

In the past decades, a wide number of scientists have developed laboratory test procedures to understand ASR-induced expansion and deterioration (micro/macro cracks formation and propagation) on affected specimens under free expansion conditions in the laboratory [5, 6]. However, it has been found that confinement differences (i.e. confined vs confined) between laboratory and field were leading to major discrepancies in the deterioration process [7].

A few research works have been performed on reinforced concrete structures to evaluate the confinement effects on ASR-induced expansion and damage development [8]. Some authors claimed that ASR overall damage cannot be lessened by adding internal and/or external reinforcement [1], while others think differently [9]. Furthermore, it has been found that major crack formation take place in a more oriented fashion in reinforced concrete (i.e. normally parallel to the main reinforcement) when compared to unconfined concrete, which normally displays a random damage pattern (i.e. map cracking). Hobbs and Swamy [10, 11] reported that the steel reinforcement controls ASR-induced crack width and pattern, along with stress distribution of damaged concrete components.

To evaluate the effects of confinement on ASR-induced expansion, Fan et al. [10] performed laboratory tests on reinforced beams and compared the result with unreinforced beams. The outcomes confirmed that induced expansions in both longitudinal and transverse directions were reduced significantly in reinforced concrete members. Giaccio et al. [2] investigated the confinement effects on ASR affected concrete using steel fibers and found that expansions and cracks width were reduced significantly. Results also indicated that mechanical properties were very close to the original values after ASR damage.

3. DIAGNOSIS OF ASR-AFFECTED CONCRETE

Numerous non-destructive and microscopic techniques were developed over the last decades to evaluate damage in ASR-affected concrete. Amongst those, some procedures stood out such as the Nonlinear Impact Resonance Acoustic Spectroscopy (NIRAS) and the Damage Rating Index (DRI), non-destructive and microscopic test methods respectively.

3.1 Non-destructive tests (NDT)

Nonlinear ultrasonic and acoustics-based methods are commonly used non-destructive techniques to appraise damage in ASR-affected concrete. These methods are found quite responsive to identify distress when compared to traditional linear acoustic methods [12–16]. Chen et al. [13] proposed a new technique based on the impulse excitation of concrete samples measuring their free vibration responses and named it as nonlinear impact resonance acoustic spectroscopy (NIRAS). The authors explained that concrete is a heterogeneous and nonlinear material by nature, hence while affected by ASR, NIRAS could recognize microcracks through the assessment of its resonance frequencies. Several authors comply with this idea, claiming that cracks are “imperfect bond systems” and thus affected material might display lessened stiffness while the resonance frequencies should escalate the nonlinear effects. This resonance frequency shift is accepted by researchers as a function of concrete macroscopic nonlinearity property to quantify damage [12-16]. As a consequence equations (1) and (2) were proposed based on this idea [12]:

$$(f_0\text{-}f)\ /f_0 = \acute{\alpha}\Delta\varepsilon \tag{1}$$

$$E = E_0\,[1 + \beta\varepsilon + \delta\varepsilon^2 + \alpha\ (\Delta\varepsilon{+}\varepsilon\mathrm{sgn}\ (\acute{\varepsilon}))] \tag{2}$$

Equation (1) represents the nonlinearity parameters where f_0 is the linear resonance frequency, f is the resonance frequency at increased excitation amplitude and $\acute{\alpha}$ is proportional to α. In addition, equation (2) parameters are: E_0 that refers the linear elastic modulus for small deformation, β represents the parameter for quadratic anharmonicity, δ refers the parameter for cubic anharmonicity, ε is strain, Δε refers the strain amplitude, α is the hysteresis nonlinearity property, $\acute{\varepsilon}$ is strain rate and sgn($\acute{\varepsilon}$)=1 if $\acute{\varepsilon}>0$; –1 if $\acute{\varepsilon}<0$; 0 if $\acute{\varepsilon}=0$ [12].

3.2 Microscopic analysis

The Damage Rating Index (DRI) is a microscopic analysis developed by Grattan-Bellew and Danay [17-20] whose main purpose is to appraise internal damage in affected concrete. The DRI is performed on polished concrete sections with the use of a stereomicroscope (with magnification approximately 15 to 16x) where damage features are counted through a 1 cm² grid drawn on the surface of a polished concrete section. Ideally, a surface of at least 200 cm² should be used, however for comparative purposes the final DRI value is normalized to a 100 cm² area. Recently, Sanchez et al. performed the DRI on concrete samples presenting different strengths and fabricated with a wide range of coarse and fine aggregates. Thus, the authors proposed a slight modification on the method, to increase its performance and reliability [20]. They suggested the use of the same weighing factors for open cracks in the aggregate particles and cement paste with or without the presence of reaction products (i.e. ASR gel). Ever since, several research works confirmed the relationship between ASR-induced expansion and DRI results. Thus, the DRI is considered to be a very effective technique for assessing ASR affected concrete regardless of the aggregate type and concrete strength [18-20].

4. SCOPE OF THE WORK

As previously discussed in the aforementioned sections, confinement effects and distinctions (i.e. confined vs 2D vs 3D scenarios) between laboratory and field concrete components may lead to significant damage differences. Yet, these distincts are not fully undertood. This work aims to understand the influence of distinct confinement scenarios on ASR-induced expansion and damage development. Concrete samples presenting two highly reactive aggregate types (fine and coarse) were fabricated, wrapped with carbon fiber reinforced polymer (CFRP), and monitored over time in the laboratory. Various confinement conditions (i.e. non-confined, 1 CFRP layer,and 2 CFRP layers) were selected for analysis and non-destructive and microscopic test procedures were conducted at distinct expansion levels. Finally, comparisons amongst the distinct confined scenarios were performed.

5. EXPERIMENTAL PROGRAM

Two highly reactive aggregates (i.e. Springhill coarse aggregate and Texas sand) were selected for this research to fabricate 35 MPa concrete specimens (100 by 200 mm cylinders). Non-reactive fine and coarse aggregates (Ottawa natural sand and non-reactive limestone) from natural quarries of Ottawa were also selected for concrete manufacturing. The coarse aggregates ranged in size from 5 to 20 mm. A conventional Portland cement (CSA Type GU, ASTM type 1) containing high alkali content (0.88% Na_2O_e) was used in the mixture. Reagent grade NaOH was used to raise the total alkali content of the mixtures to 1.25% Na_2O_e by cement mass, for accelerating AAR expansion process.

A total of 108 concrete cylinders (i.e. 54 per aggregate type), 100 by 200 mm in size were fabricated using the two highly reactive aggregates presented above. After 24 hours, the specimens were demoulded and moist cured for over 24 hours. Carbon fiber reinforced polymer (CFRP) was selected to provide the concrete specimens with different confinement scenarios (Figure 5.1(a)), depending upon the number of layers applied. Three scenarios were selected for assessment within the project: 1) non-confined; 2) wrapping with 1 CFRP layer applied before ASR development and maintained over testing and, 3) wrapping with 2 CFRP layers applied before ASR development and maintained over testing. The CFRP sheets were glued on the concrete samples using an epoxy coating.

Small holes, 5 mm in diameter by 15 mm long, were then drilled in both ends of each test specimen and stainless-steel gauge studs were glued in place, with a fast setting cement slurry for longitudinal expansion measurements. After the completion of the first 72 h (i.e. three days from casting), the zero reading was conducted, and the specimens were stored in conditions (Figure 5.1(b)) enabling ASR development (i.e. 38°C and 100% R.H.) and monitored over time. Four levels of expansion (or damage) were selected for further analysis: 0.05% (low); 0.12% (moderate); 0.20% (high) and 0.30% (very high). Once the test specimens reached the above expansion levels, they were wrapped in plastic film and stored at 12°C to stop ASR further development until non-destructive and microscopic tests were conducted.

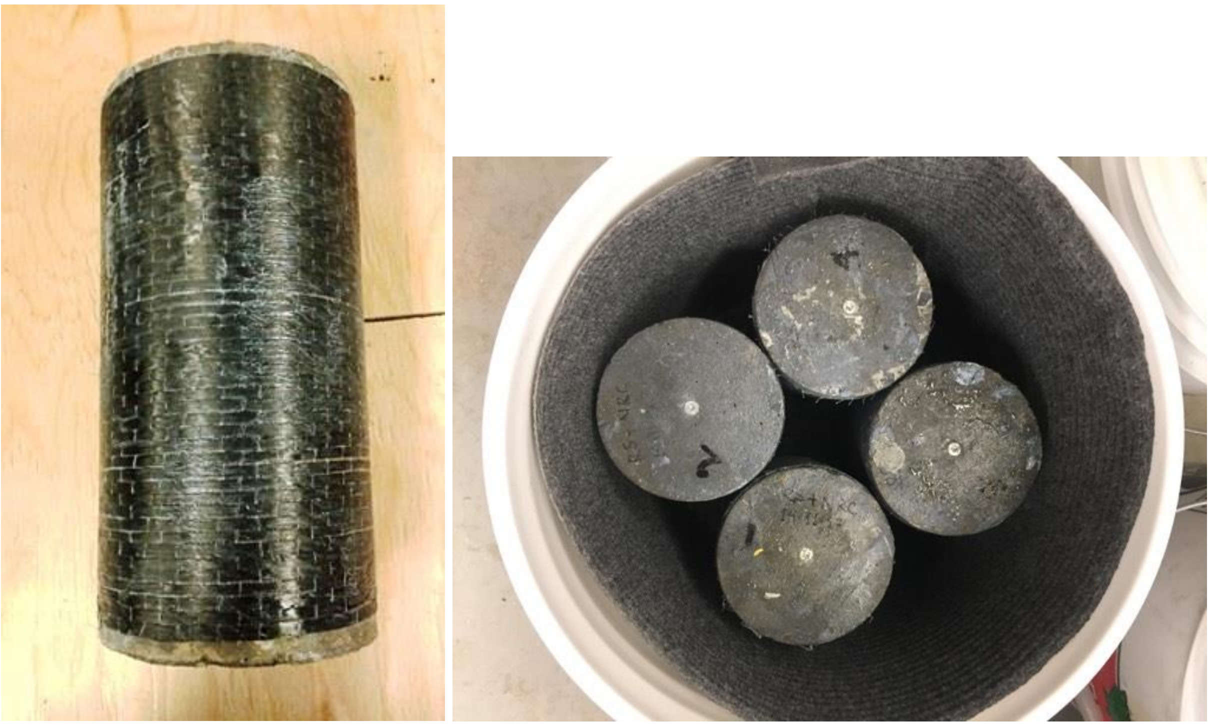

(a) (b)

Figure 5.1: Fabrication and conditioning: a) Concrete sample wrapped with CFRP and b) Storage condition of the concrete samples.

5.1 Concrete assessment and analysis

The specimens were unwrapped just before testing and expansion readings were taken to confirm that no outstanding expansion (and or shrinkage) took place during the storage period. Nonlinear impact resonance acoustic spectroscopy (NIRAS) and Damage Rating Index (DRI) were then performed on test specimens containing coarse and fine reactive aggregates and distinct expansion levels.

5.1.1 Nonlinear Impact Resonance Acoustic Spectroscopy (NIRAS) technique

To perform the test, the studs from all evaluated specimens were completely removed from their ends. Then, the specimens were placed on a supporting mat and connected to a high frequency accelerometer using a quick setting adhesive which is combined with an oscilloscope (Figure 5.2). The specimens were vibrated at the center with a low amplitude hammer stimulating the transverse flexural vibration mode. This vibration spreads to the entire specimen and evaluates its inner condition, being recorded by the oscilloscope connected to the accelerometer. The Fast Fourier Transform (FFT) is then used to acquire the vibration signals and frequency spectrum. At least 10 individual impacts of different strength were applied on each specimen to interpret the difference in resonance frequency. The analysis is conducted according to the resonance frequency and impact amplitude as follows: the greater the damage, the lower the resonance frequency and the higher the impact amplitude [15].

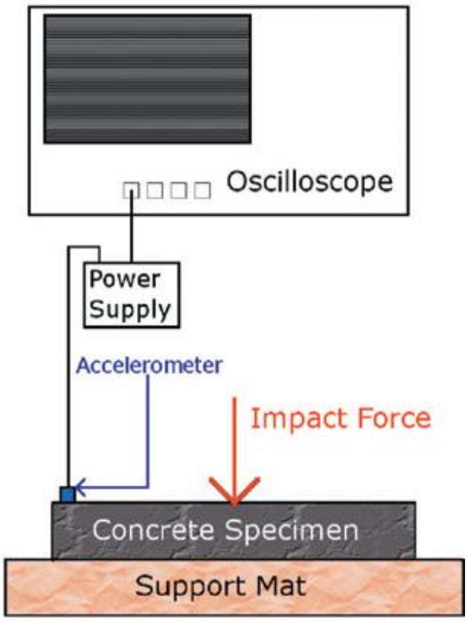

Figure 5.2: Schematic setup of NIRAS test [15].

5.1.2 Damage rating Index (DRI)

One specimen per expansion level per reactive aggregate was taken out from the 12°C storage, and its steel studs were completely removed. Then, the specimens were cut in two, axially, and one of the flat surfaces was polished using a standard polishing device which uses diamond-impregnated rubber disks (No 50 [coarse], 100, 400, 800, 1500, 3000 [very fine]); this device was found most suitable for the work, as it does not loose abrasive powders that can fill up cracks or voids in concrete, and high quality polishing is obtained with minimal water supply so that ASR-gel leaching is avoided. Afterwards, the DRI was performed as per Sanchez et al. [6].

6. RESULTS

6.1 AAR-induced Expansion

The results for ASR-induced expansion as a function of time are presented for the three different confinement states (i.e. unconfined, wrapped with 1 and 2 CFRP layers) and for concrete incorporating two reactive aggregate types (i.e. Texas sand and Springhill coarse aggregate). Figure 6.1 (a) illustrates the expansion measurements gathered for samples fabricated with the reactive Texas sand (Tx) whereas Figure 6.1 (b) displays the results for specimens proportioned with the reactive Springhill (Sp) coarse aggregate.

Analyzing the plots, it can be observed that slightly faster ASR kinetics was found for the samples fabricated with the Tx sand when compared to Sp coarse aggregate whatever is the test condition, as expected and reported in previous researches. Furthermore, non-confined specimens presented much faster expansion kinetics (and higher expansion levels achieved over time) when compared to the 1 and 2 layers of CFRP wrapping, whereas confined specimens displayed quite close expansion development regardless the number of CFRP layers (specimens wrapped with 2 layers presented slightly faster kinetics). Very high expansion (0.3%) was reached at 350 days for concrete samples fabricated with Texas sand and wrapped with 2 layers of CFRP, while at 410 days for samples made of Springhill coarse aggregate. The same expansion level was reached at 440 and 500 days for samples wrapped with two layers and made of Tx and Sp aggregates, respectively.

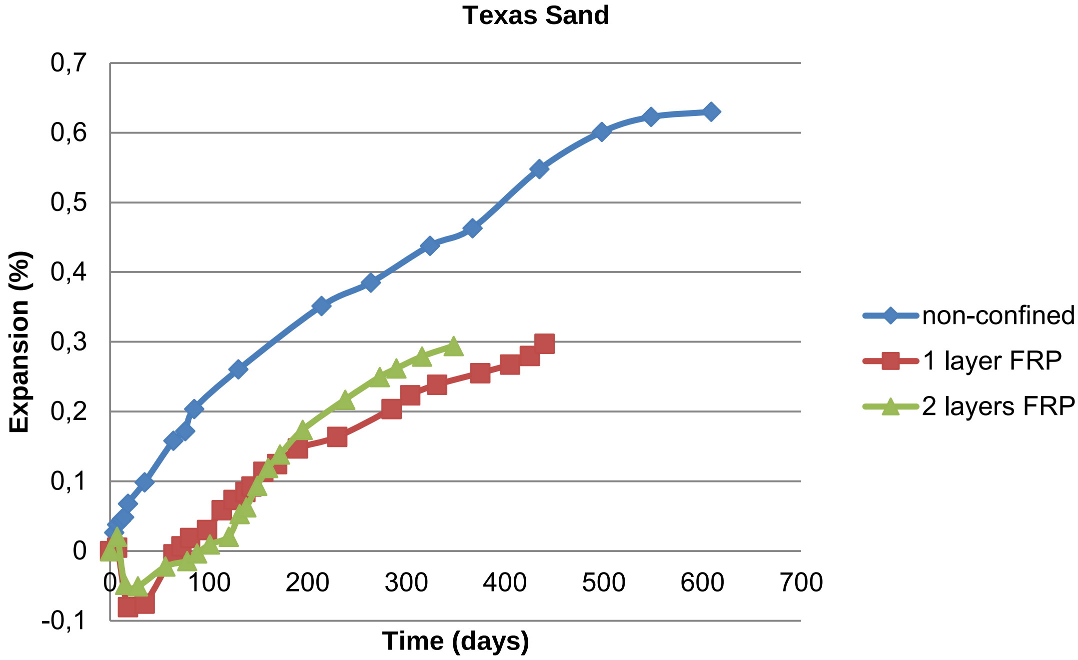

(a)

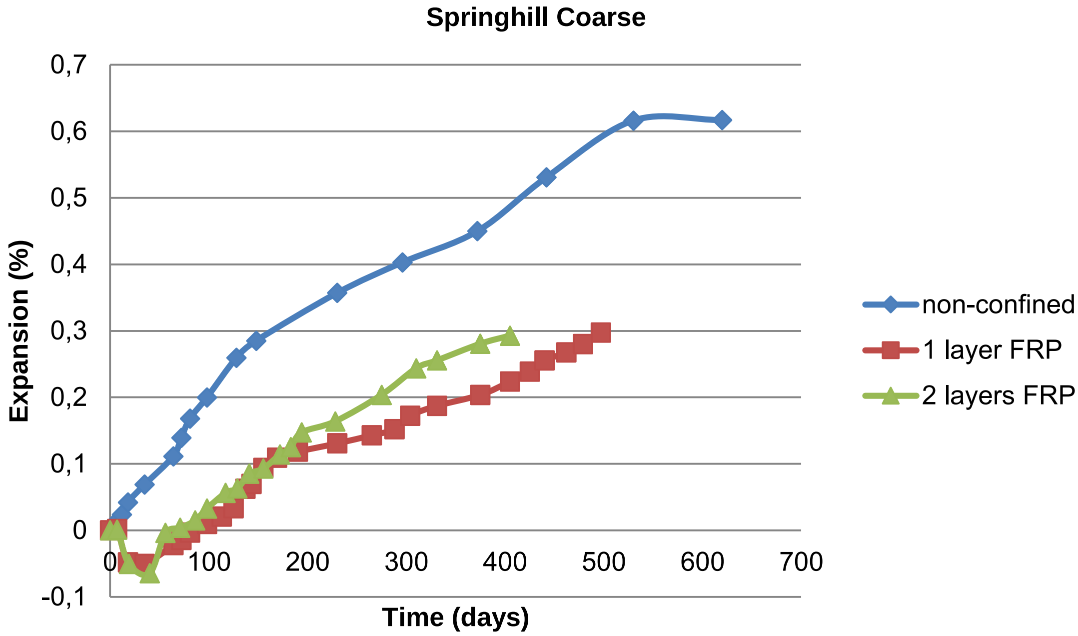

(b)

Figure 6.1: Expansion vs. time obtained for concrete tested with different confined state incorporating (a) reactive Texas sand, and (b) reactive Springhill coarse aggregate.

6.2 Nonlinear Impact Resonance Acoustic Spectroscopy (NIRAS) technique

The results from NIRAS test on concrete specimens wrapped with 1 layer CFRP can be observed in Figure 6.2 (a-d) for Texas sand. It is anticipated that NIRAS test appraises microcracks and damage in concrete through resonance frequency shift and impact amplitude. A number of studies demonstrated that the lower the resonance frequency and the higher the impact amplitude, the higher the concrete damage [12-19].

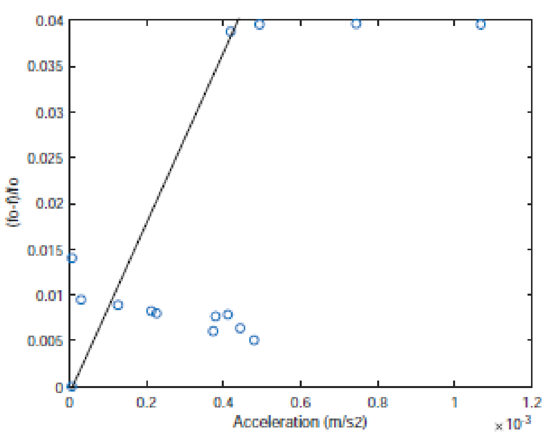

(a) Texas sand, 1 layer, 0.05% expansion

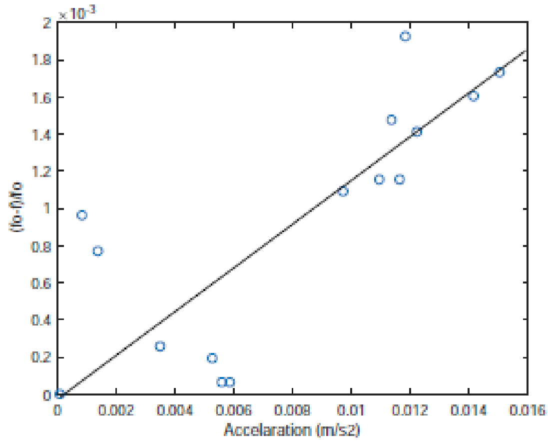

(b) Texas sand, 1 layer, 0.12% expansion

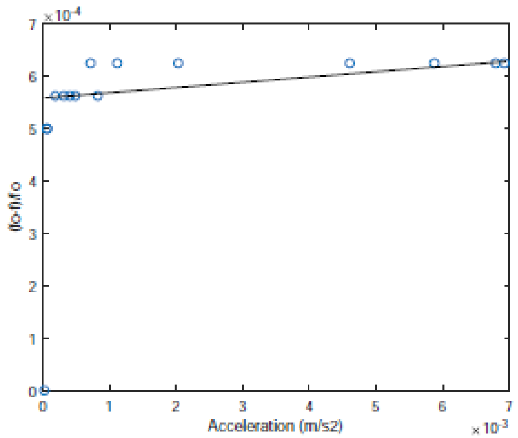

(c) Texas sand, 1 layer, 0.20% expansion

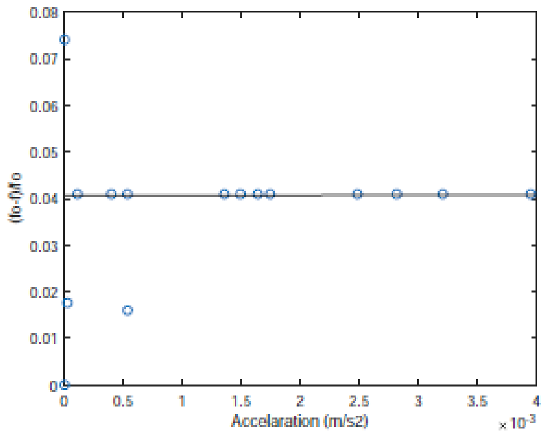

(d) Texas sand, 1 layer, 0.30% expansion

Figure 6.2: Nonlinearity comparison of specimens at different confined states and selected expansion levels (Texas sand)

It is noticed from the data above that at lower expansion levels (i.e. 0.05%), the nonlinearity curve is very steep which means that ASR-damage is well captured. As the expansion level increases, the nonlinearity curve (i.e. curve slope) becomes less steep. From 0.20% expansion and onwards, the nonlinearity curve becomes flat, which indicates that NIRAS is not suitable to capture damage from this reaction stage. The nonlinearity graphs of the two other confined states (i.e. non-confined and specimens wrapped with 2 layers CFRP) followed a very similar pattern of the presented above for both types of aggregates.

6.3 Damage Rating Index (DRI)

The results of petrographic analysis in terms of DRI numbers as a function of ASR-induced expansions are presented in Figure 6.3. It can be observed that the DRI number increases as the expansion level rises, for non-confined and both confinement states; indicating that the higher the expansion level, the greater the damage degree, as expected. The number of closed cracks in the aggregate particles (CCA) does not increase with the raise in expansion, since it is not considered as a distress feature linked to ASR-induced development. However, the open cracks in the aggregate particles (without or with reaction products - OCA and OCAG) and the cracks in cement paste (without or with gel - CCP and CCPG) indeed increase as a function of induced expansion.

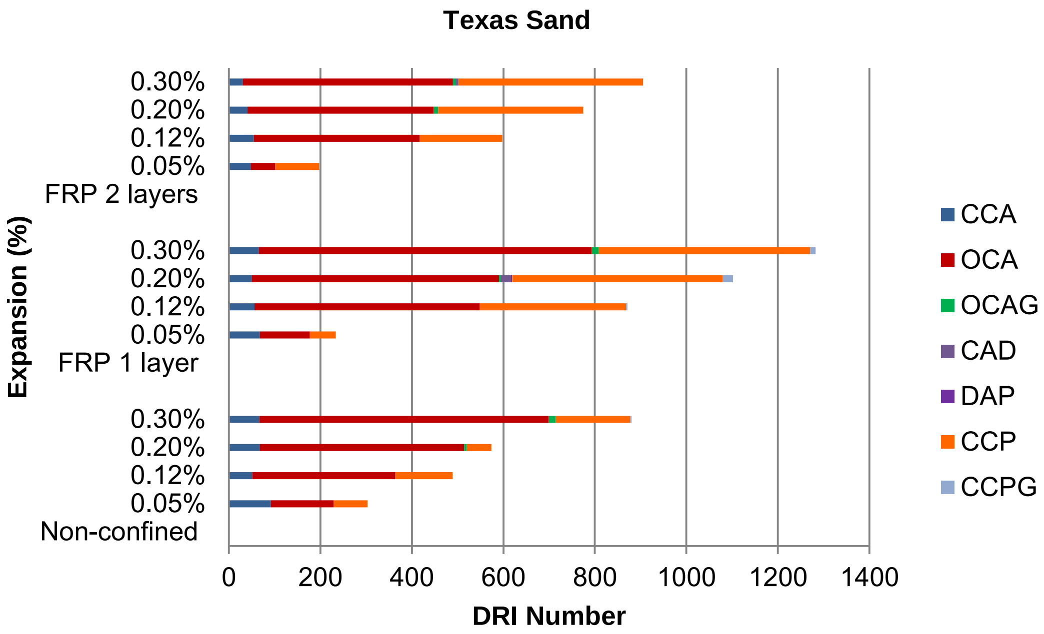

(a)

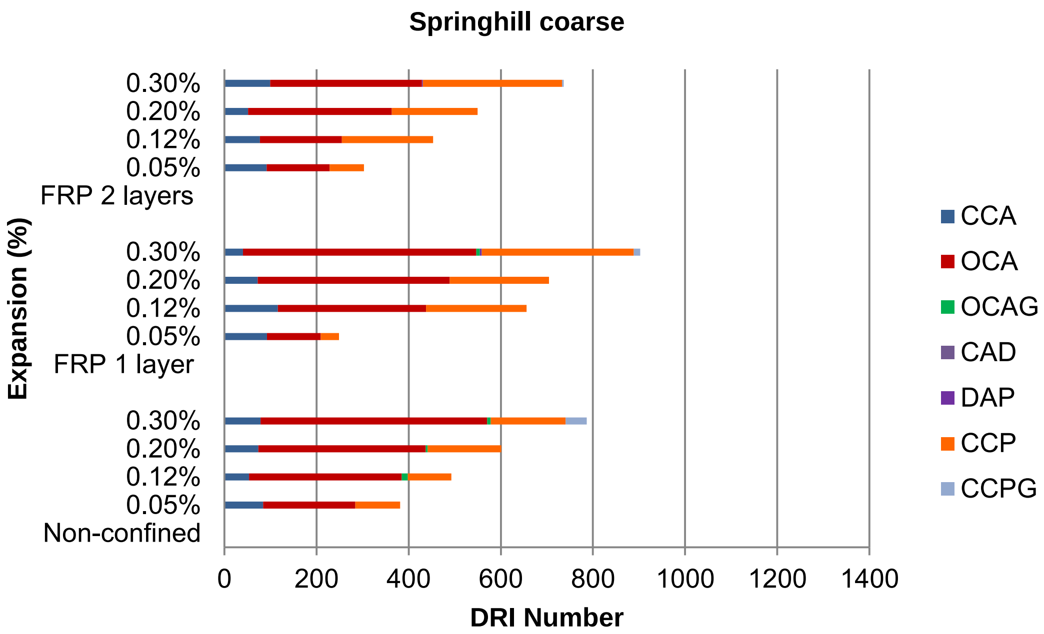

(b)

Figure 6.3: DRI numbers of concrete specimens in different confined states using reactive sand and coarse aggregates.

Comparing the results presented above, it is clear that that the confinement effect causes differences in the DRI number of affected samples at the same expansion levels. For Tx sand, the unconfined specimens presented the lowest damage degree for all expansion levels selected for analysis, followed by the 2 layers wrapping and finally the 1-layer wrapping, displaying the highest distress degree. Likewise, for Sp mixtures the non-confined specimens also demonstrated the lowest amount of damaged. Yet, for this aggregate type very similar results were obtained for unconfined and 2 layers. However, similar to Tx sand, the highest values were obtained for 1-layer CFRP layer.

7. DISCUSSION

The expansion vs. time plot presented in Figure 6.1 compares and evaluates the variations in expansion for the different confined and non-confined states appraised. It can be noted that a much longer period of time (more than 1 year) was required for the wrapped specimens to reach the highest expansion level selected for analysis in this work (i.e. 0.30%) for both highly reactive aggregates used. Yet, the non-confined specimens experienced faster ASR kinetics and reached 0.30% expansion level at very early ages (about 200 days). The latter seems to indicate that confinement may indeed delay ASR-induced development; however, this work may not conclude whether the confinement might also decrease ASR ultimate expansion since the test of the confined samples was stopped after 0.30% expansion.

Since kinetics was found to be different between unconfined and confined specimens, non-destructive (NIRAS) and microscopic (DRI) techniques were also conducted to check whether at the same level of expansion, differences on the deterioration pattern and or degree could be observed. Unfortunately, NIRAS results demonstrated that this test is only responsive to detect induced cracks and damage at early stages of the deterioration process (i.e. lower - 0.05% and moderate - 0.12% expansion levels). However, the procedure showed to be inaccurate to detect damage progression at high (i.e. 0.20%) and very high (0.30%) expansion levels for all aggregate types and confined states. Therefore, no comparisons could be made amongst the distinct confinement scenarios studied. It is worth noting that at high and very high levels of induced expansion and deterioration, ASR distress process presents a large number of open cracks within the aggregate particles and cement paste. Moreover, from this point and onwards the amount of reaction products (i.e. ASR gel) increases significantly within the reactive aggregates and in the cement paste. Therefore, the presence of reaction products may somehow harm NIRAS precision to accurately detect ASR net cracking formation and expansion level.

The DRI numbers (Figure 6.3) obtained in this work showed distinct values for specimens presenting the same expansion level but different confinement configurations. Overall, the DRI numbers ranged from about 250 for low expansion levels (i.e. 0.05%) to about 1300 for very high expansion levels (i.e. 0.30%) for both aggregate types. The DRI numbers of unconfined specimens were close to the range of 2 layers of CFRP, yet the latter one experienced more cracks in cement paste. However, the number of cracks in the cement paste (without or with gel – CCP and CCPG) for the specimens wrapped with 1 layer of CFRP were higher when compared to the unconfined and 2 CFRP layers specimens. Moreover, not only the amount of cracks changed but also the crack pattern, since CFRP wrapped samples, especially with 2 layers, displayed a significant amount of cracks in the cement paste aligned with the direction of the confinement as experienced by real structures and reported in [10, 11].

Following the assessment of the microscopic features discussed above, and especially due to the differences in cracking pattern presented by the 2 layer CFRP samples, a qualitative and descriptive model for ASR-induced damage development under confined states is proposed in this work (Figure 7.1) and presented as follows: at early stages (i.e. 0.05%), cracks are mainly formed within the aggregate particles and they start running out to the cement paste at moderate levels of expansion (i.e. 0.12%). At this level, the induced distress development follows roughly the same pattern of unconfined samples, except that the generated cracks tend to be parallel to the main confinement direction (i.e. along the main specimen direction – 200 mm). At high expansion levels (i.e. 0.20%), these cracks previously formed in the aggregates reach completely the cement paste at both sides of the aggregates and start linking to each other, forming an extensive cracking network. Finally, at very high expansion levels (i.e. 0.30%) multiple cracks are seen completely linked to each other, mostly parallel to the sample's edge.

The description above differentiates quite a lot from the model proposed by [6] and illustrated in Figure 7.2, which confirms that not only ASR kinetics is changed with the presence of confinement, but also ASR-induced deterioration changes too. Moreover, although mechanical testing has not been conducted so far in this project, it is anticipated that a major impact will take place on the mechanical response of confined ASR-affected specimens since not only the number but rather the damage propagation pattern is fairly different.

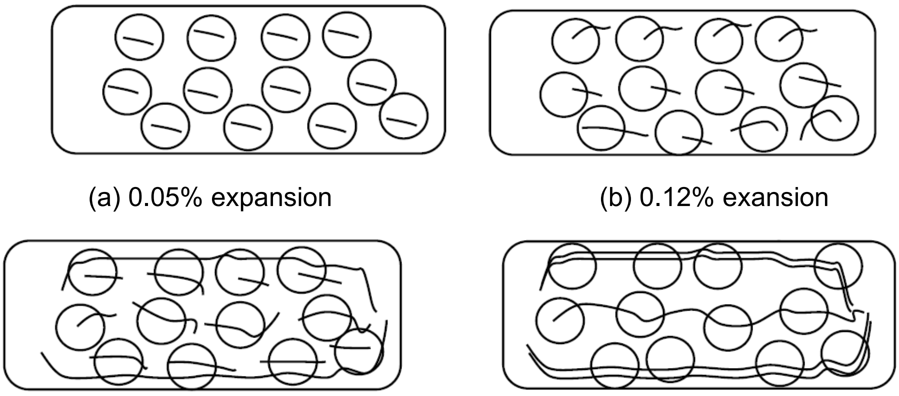

(a) 0.05% expansion (b) 0.12% exansion

(c) 0.20% expansion (d) 0.30% expansion

Figure 7.1: AAR damage model for 2 layers confined specimens at various expansion level.

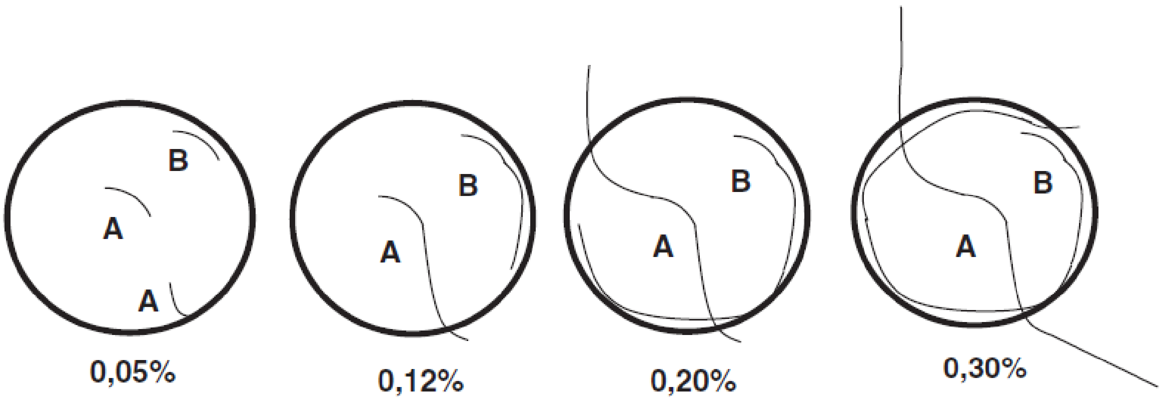

Figure 7.2: Qualitative AAR-induced damage model for affected specimens under free expansion at different expansion levels as per [6]

8. CONCLUSION

The main objective of this study was to better understand the effects of confinement on ASR-induced expansion and damage. The main findings observed in this work are presented hereafter:

- Unconfined affected concrete specimens seem to display an ASR-induced development much faster than confined samples, either with 1 or 2 layers of CFRP and regardless of the reactive aggregate type used. The latter indicates that indeed confinement changes (i.e. delays) ASR-induced expansion development. However, conclusions could not be taken on the impact of confinement on ASR ultimate expansion since test of the confined samples stopped after 0.30% expansion;
- The NIRAS test has been found effective to understand and detect the damage degree up to moderate level (0.12%); yet, the method showed to be inaccurate to appraise ASR-affected concrete at high and very high induced expansion and distress levels regardless of the confined state and aggregate type used. Therefore, further comparisons on the effect of damage as a function of the confinement configuration could not be performed using this procedure;
- The DRI was found very effective to evaluate ASR-induced expansion and deterioration though. Moreover, important differences in petrographic damage features were found as a function of the confinement scenario. Confined samples presented overall higher number of cracks (especially in the cement paste) when compared to unconfined ones for the same level of expansion. The worst-case scenario was obtained for specimens with 1 layer of CFRP, which cannot be completely explained at this stage. Yet, it seems evident that for the same expansion level, damage is quite different in restrained vs. non-restrained conditions;

- A qualitative and descriptive model is proposed in this work. The latter evidences very distinct features (i.e. higher amount of cracks in the cement paste) and pattern (cracks aligned/parallel to the main confinement direction) of samples affected by ASR under confinement scenarios when compared to samples damaged under free expansion as per the model proposed by [6].
- Although mechanical techniques have not been conducted so far in this project, it is anticipated that the confinement may bring a significant impact on the mechanical response of affected concrete, especially due to the important pattern change observed. Further analysis is still required in this regard.

9. REFERENCES

[1] Fournier, B., & Bérubé, M. A. (2000). Alkali-aggregate reaction in concrete: a review of basic concepts and engineering implications. Canadian Journal of Civil Engineering, 27(2), 167-191.

[2] Giaccio, G., Bossio, M. E., Torrijos, M. C., & Zerbino, R. (2015). Contribution of fiber reinforcement in concrete affected by alkali–silica reaction. Cement and Concrete Research, 67, 310-317.

[3] Kubat, T., Al-Mahaidi, R., & Shayan, A. (2016). CFRP confinement of circular concrete columns affected by alkali-aggregate reaction. Construction and Building Materials, 116, 98-109.

[4] Broekmans, M. A. T. M. (2002). The alkali-silica reaction: mineralogical and geochemical aspects of some Dutch concretes and Norwegian mylonites (Doctoral dissertation).

[5] HAFÇI, A. (2013). Effect of alkali–silica reaction expansion on mechanical properties of concrete. Middle East Technical University, 1-116.

[6] Sanchez, L. F. M., Fournier, B., Jolin, M., & Duchesne, J. (2015). Reliable quantification of AAR damage through assessment of the Damage Rating Index (DRI). Cement and Concrete Research, 67, 74-92.

[7] Wen, H. X. (1993). Prediction of structural effects in concrete affected by alkali-aggregate reaction.

[8] Danay, A. (1994). Structural Mechanics Methodology in Diagnosing and Assessing Long-Term Effects of AAR in R/C Structures. Materials Journal, 91(1), 54-62.

[9] Fan, S., & Hanson, J. M. (1998). Effect of alkali silica reaction expansion and cracking on structural behavior of reinforced concrete beams. ACI Structural Journal, 95, 498-505.

[10] Swamy, R. N. (1995, October). Effects of alkali aggregate reactivity on material stability and structural integrity. In Proceedings of the CANMET/ACI International Workshop on Alkali–Aggregate Reactions in Concrete, Dartmouth, Nova Scotia (pp. 1-4).

[11] Hobbs, D.W. 1988. Alkali–silica reaction in concrete. Thomas Telford, London, U.K., p. 83.

[12] Leśnicki, K. J., Kim, J. Y., Kurtis, K. E., & Jacobs, L. J. (2011). Characterization of ASR damage in concrete using nonlinear impact resonance acoustic spectroscopy technique. NDT & E International, 44(8), 721-727.

[13] Chen, X. J., Kim, J. Y., Kurtis, K. E., Qu, J., Shen, C. W., & Jacobs, L. J. (2008). Characterization of progressive microcracking in Portland cement mortar using nonlinear ultrasonics. NDT & E International, 41(2), 112-118.

[14] Chen, J., Jayapalan, A. R., Kim, J. Y., Kurtis, K. E., & Jacobs, L. J. (2010). Rapid evaluation of alkali–silica reactivity of aggregates using a nonlinear resonance spectroscopy technique. Cement and Concrete Research, 40(6), 914-923.

[15] Buck, O., Morris, W. L., & Richardson, J. M. (1978). Acoustic harmonic generation at unbonded interfaces and fatigue cracks. Applied Physics Letters, 33(5), 371-373.

[16] Solodov, I. Y., & Korshak, B. A. (2001). Instability, chaos, and “memory” in acoustic-wave–crack interaction. Physical review letters, 88(1), 014303.

[17] Sanchez, L. F. M., Fournier, B., Jolin, M., & Bastien, J. (2014). Evaluation of the stiffness damage test (SDT) as a tool for assessing damage in concrete due to ASR: test loading and output responses for concretes incorporating fine or coarse reactive aggregates. Cement and concrete research, 56, 213-229.

[18] Sanchez, L. F. M., Fournier, B., Jolin, M., & Bastien, J. (2015). Evaluation of the Stiffness Damage Test (SDT) as a tool for assessing damage in concrete due to alkali-silica reaction (ASR): Input parameters and variability of the test responses. Construction and building Materials, 77, 20-32.

[19] Villeneuve, V., Fournier, B., & Duchesne, J. (2012, May). Determination of the Damage in Concrete Affected by ASR—the Damage rating Index (DRI). In 14th International Conference on Alkali-Aggregate Reaction (ICAAR). Austin, Texas (USA).

[20] Sanchez, L. F. M., Fournier, B., Jolin, M., & Duchesne, J. (2015). Reliable quantification of AAR damage through assessment of the Damage Rating Index (DRI). Cement and Concrete Research, 67, 74-92.